The British Journal of Radiology, 85 (2012), 887–896

REVIEW ARTICLE

CT and MR cholangiography: advantages and pitfalls in perioperative evaluation of biliary tree

[1]T HYODO, MD, [1]S KUMANO, MD, [2]F KUSHIHATA, MD, [1]M OKADA, MD, PhD, [3]M HIRATA, MD, [4]T TSUDA, MD, [2]Y TAKADA, MD, [4]T MOCHIZUKI, MD and [1]T MURAKAMI, MD, PhD

[1]*Department of Radiology, Kinki University Faculty of Medicine, Osaka-Sayama, Osaka, Japan,* [2]*Department of Hepato-biliary-pancreatic Surgery and Transplantation, Ehime University Graduate School of Medicine, Toon, Ehime, Japan,* [3]*Department of Radiology, Matsuyama Red Cross Hospital, Matsuyama, Ehime, Japan, and* [4]*Department of Diagnostic and Therapeutic Radiology, Ehime University Graduate School of Medicine, Toon, Ehime, Japan*

ABSTRACT. Recent developments in imaging technology have enabled CT and MR cholangiopancreatography (MRCP) to provide minimally invasive alternatives to endoscopic retrograde cholangiopancreatography for the pre- and post-operative assessment of biliary disease. This article describes anatomical variants of the biliary tree with surgical significance, followed by comparison of CT and MR cholangiographies. Drip infusion cholangiography with CT (DIC-CT) enables high-resolution three-dimensional anatomical representation of very small bile ducts (*e.g.* aberrant branches, the caudate branch and the cystic duct), which are potential causes of surgical complications. The disadvantages of DIC-CT include the possibility of adverse reactions to biliary contrast media and insufficient depiction of bile ducts caused by liver dysfunction or obstructive jaundice. Conventional MRCP is a standard, non-invasive method for evaluating the biliary tree. MRCP provides useful information, especially regarding the extrahepatic bile ducts and dilated intrahepatic bile ducts. Gadolinium ethoxybenzyl diethylenetriamine pentaacetic acid-enhanced MRCP may facilitate the evaluation of biliary structure and excretory function. Understanding the characteristics of each type of cholangiography is important to ensure sufficient perioperative evaluation of the biliary system.

Received 20 November 2010
Revised 21 August 2011
Accepted 6 September 2011

DOI: 10.1259/bjr/21209407

Despite recent technical advances in surgical procedures [1, 2], competent surgery for biliary disease remains difficult. The reasons include the invasive nature of malignant tumours of the biliary tract and the complex anatomy of the portal and biliary systems. In addition, the biliary tree has a high frequency of variations. Misidentification of biliary anatomy can result in complications involving not only perioperative management, but also patient prognosis. Biliary tract complications after orthotopic liver transplantation have been reported in 10–25% of cases, proving fatal in up to 10% of complicated cases [3, 4]. Laparoscopic cholecystectomy is a less invasive procedure, but the limited visual field and errors of misperception occasionally result in biliary complications such as bile leakage and injury to the contralateral biliary ducts (approximately 0.5% of cases) [3, 4]. Thus, precise knowledge of anatomical variations of the biliary system and careful pre-operative evaluation are key to safe and satisfactory excision.

In recent years, the rapid development of CT and MRI have provided high-resolution imaging and have contributed to planning for hepatobiliary surgery and post-operative evaluation for suspected complications. The volume data allow the acquisition of arbitrary cross-sectional planes or other three-dimensional (3D) imaging, which is effective to visually grasp the complex anatomy of the bile duct: volume rendering (VR) provides a stereoscopic view of the course of the biliary tree, while maximum-intensity projection (MIP) images appear less 3D but give better visualisation of tiny bile ducts such as the caudate branch. Thus, these imaging modalities can be good alternatives to endoscopic retrograde cholangiopancreatography or direct cholangiography [5, 6]. Throughout the world, MR cholangiopancreatography (MRCP) plays a central role in evaluation of the biliary system. Meanwhile, drip infusion cholangiography with CT (DIC-CT) is becoming less common because the market for intravenous cholangiographic contrast media is limited to a few countries. However, DIC-CT has been shown to provide high-quality images of the biliary system in previous studies.

This article first describes anatomical variants of the hepatic hilar bile ducts and the cystic duct with surgical significance. We then refer to the advantages and disadvantages of DIC-CT and conventional MRCP for evaluating the biliary system. The potential utility of contrast-enhanced MR cholangiography with gadolinium ethoxybenzyl

Address correspondence to: Dr Tomoko Hyodo, Department of Radiology, Kinki University Faculty of Medicine, 377-2 Ohno-higashi, Osaka-Sayama, Osaka 589-8511, Japan. E-mail: hyoudou@radiol.med.kindai.ac.jp

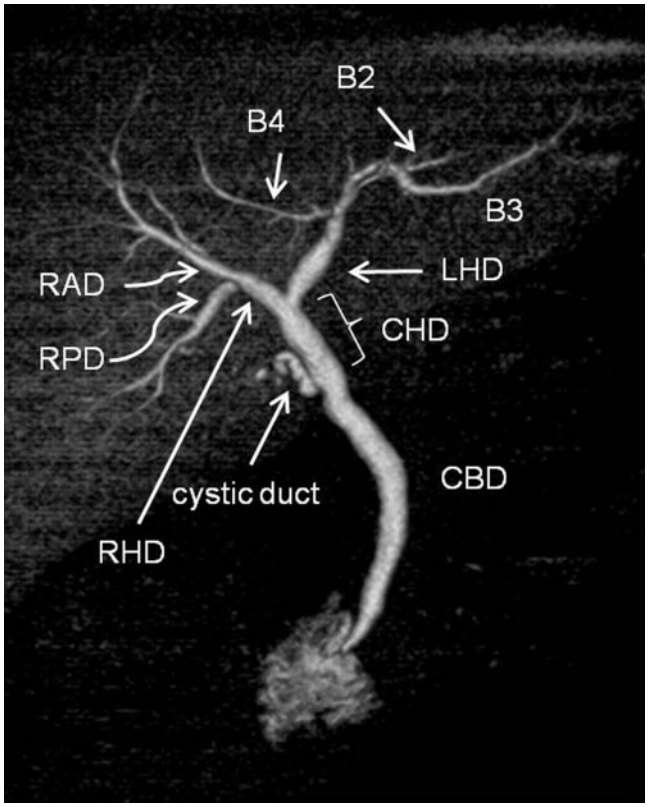

Figure 1. Volume rendering image from drip infusion cholangiography with CT shows conventional branching pattern of the biliary tree in a 71-year-old male with acute cholecystitis. There is no filling of the gallbladder due to cystic duct obstruction. B2, segment II bile duct; B3, segment III bile duct; B4, segment IV bile duct; CBD, common bile duct; CHD, common hepatic duct; LHD, left hepatic bile duct; RAD, right anterior duct; RHD, right hepatic duct; RPD, right posterior duct.

diethylenetriamine pentaacetic acid (Gd-EOB-DTPA; Primovist, Bayer Schering Pharma) is also discussed.

Anatomical variants of the biliary tree

In this section, the anatomical variations of the hilar bile ducts (including the branches of the caudate lobe) and the cystic duct are discussed using high-resolution DIC-CT images. Figure 1 shows the normal anatomy of the biliary system. Traditionally, liver surgery relies on Couinaud's liver segment classification [7]. The right anterior duct drains Couinaud's segments V and VIII, and the right posterior duct drains segments VI and VII. The right hepatic duct is formed by the fusion of the anterior duct and the posterior duct. The left hepatic duct drains segments II, III and IV. The right and left hepatic bile ducts form the hilar bile ducts, which merge to form the common hepatic duct (CHD). The CHD then joins the cystic duct, which leads from the gallbladder (GB), to form the common bile duct (CBD).

Patterns of the left hepatic bile duct

Confluence patterns of B2, B3 and B4 (the bile ducts of Couinaud's segments II–IV, respectively) in the left lobe of the liver can be classified into three main types [8–10] (Figure 2, Table 1): Type A, in which the common trunk of B2 and B3 joins B4 (Figure 3); Type B, which shows a triple confluence of B2, B3 and B4; and Type C, in which B2 joins the common trunk of B3 and B4. Left hepatic ducts reportedly run supraportally in 97% of cases [9]. Kawarada et al [11] reported that B4 joined the left hepatic duct close to the hilar confluence in 35.5% of 141 liver specimens, which needs the extended liver resection for patients with hilar bile duct carcinoma. For patients undergoing right hepatic lobectomy, pre-operative recognition of these branching patterns is crucial to avoid bile duct injury.

Patterns of the right hepatic bile duct

Various reports have described the branching pattern of the right hilar bile duct [9, 12–15]. Classification according to the site of insertion of the right posterior duct is considered as the most comprehensive and useful (Figure 4, Table 2): Type 1, the most common form, is defined as the right posterior duct draining into the right anterior duct to form a right hepatic bile duct; Type 2, in which trifurcation of the right posterior, right anterior and the left hepatic bile ducts join at the same point to form the common hepatic duct (Figure 5a); Type 3, in which the right posterior duct drains into the left bile duct; and Type 4, in which the right posterior duct drains directly into the common hepatic duct (Figure 5b) [13]. Potential causes of surgical complications include the following: an infraportal course of the right posterior duct in the Type 1 pattern [9]; a right posterior duct draining into the left hepatic duct distant to the hepatic hilum in the Type 3 pattern [16]; and an aberrant right posterior duct draining into the CBD immediately above or near the confluence of the cystic duct in the Type 4 pattern [17, 18].

In adult-to-adult liver transplantation, evaluating the anatomy of the right hepatic bile duct is important for the selection of donors and accurate pre-operative planning. For example, the Type 2 pattern is considered a contraindication for safe right hepatectomy in liver

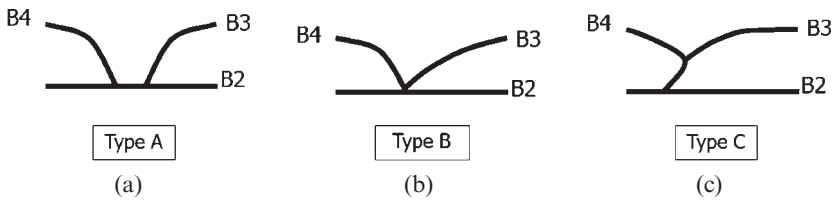

Figure 2. Schematic diagram of three confluence patterns in the left lobe of the liver. (a) Type A, where the common trunk of B2 and B3 joins B4. (b) Type B, representing a triple confluence of B2, B3 and B4. (c) Type C, where B2 joins the common trunk of B3 and B4. B2–B4, bile ducts of Couinaud's liver segments II–IV, respectively.

Table 1. Branching patterns of the left hepatic bile duct

Configuration	Description	Kitami et al [9][a] (n=202)	Ohkubo et al [8][b] (n=110)	Cho et al [10][a] (n=27)
Type A	Common trunk of B2 and B3 joins B4	69%	80%	59%
Type B	Triconfluence of B2, B3 and B4	6%	4%	11%
Type C	B2 drains into common trunk of B3 and B4	20%	16%	33%
Other	Other	5%	–	–

B2, segment II bile duct; B3, segment III bile duct; B4, segment IV bile duct.
[a]Results of four- or eight-detector row CT.
[b]Results of four- or eight-detector row operative cases.

donor candidates. This variant requires additional biliary anastomoses in the recipient that can lead to an increased risk of biliary complications [19]. Also, the right posterior duct draining into the left bile duct in the Type 3 pattern is a contraindication for both right and left liver donation. In left side hepatectomy, the Type 3 pattern is crucial to prohibit the right posterior duct injury.

Assessment of the caudate branches

The caudate lobe, consisting of the Couinaud's segments I and IX, is defined anatomically as the area supplied by the first branches of the left or right portal veins [7, 20, 21]. Kumon [22] first divided the caudate lobe into three areas based on the portal blood supply: the Spiegel lobe, the paracaval portion and the caudate process [22–25]. Resection of the caudate lobe is technically challenging, since this subsegment is located deep within the liver and is close to hepatic hilar structures [26, 27]. DIC-CT can provide information regarding the biliary branching pattern of the caudate lobe (Figures 6 and 7), which enables the surgeons to plan optimal resection and avoid post-operative complications in patients with hilar malignancies [28]. Figure 8 shows a case of hilar cholangiocarcinoma involving the left hepatic duct and paracaval branch of the caudate lobe. In this case, intravenous contrast-enhanced CT and DIC-CT revealed that all detectable biliary branches of the caudate lobe were confluent with the left hepatic duct system. Based on anatomical information and expected remnant liver volume, the surgeons achieved complete curative resection by left hepatectomy with en bloc caudate lobectomy using a left-sided approach to preserve the right hepatic lobe.

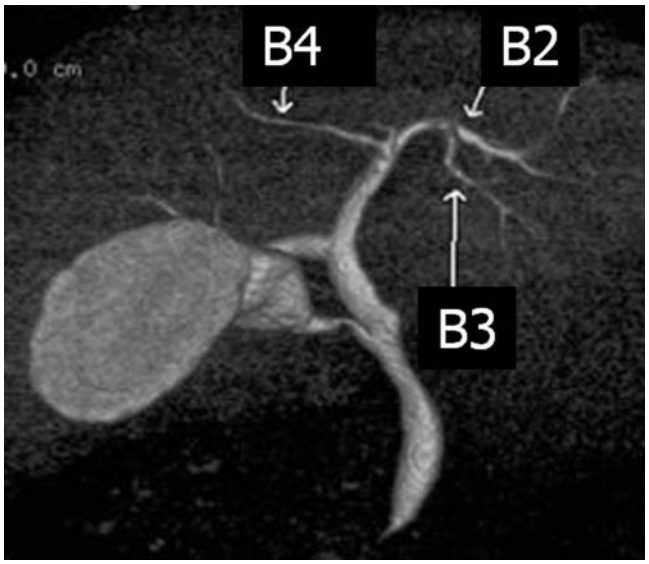

Figure 3. Volume rendering image (anterior view) from drip infusion cholangiography with CT demonstrates Type A bile duct in the left lobe of the liver. The common trunk of B2 and B3 joins B4.

Variation of the cystic duct

Pre-operative evaluation of the cystic duct is particularly important for laparoscopic cholecystectomy. The reason is that the poor visualisation of the surgical field may cause accidental bile duct injury, a rare but potentially severe complication [3, 17, 29, 30]. The cystic duct usually inserts into the middle third of the extrahepatic duct [29]. Benson and Page [31] defined five surgically important extrahepatic ductal anomalies on the basis of 205 dissections (Table 3): the four variations of the cystic duct (Types A, B, D and E); and existence of an accessory hepatic duct (Type C; see the following section on aberrant bile ducts and accessory

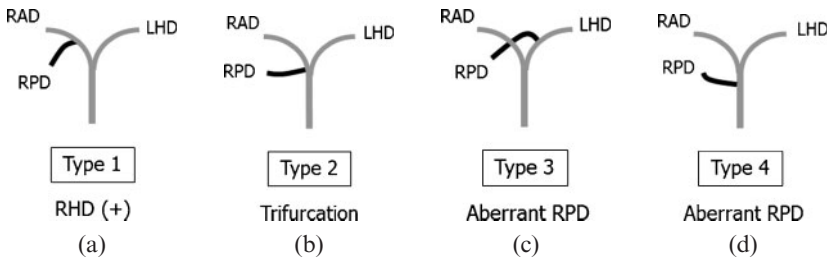

Figure 4. Schematic diagram of four variants of the right hilar bile duct. (a) Type 1, the most common type, defined as the right posterior duct (RPD) draining into the right anterior duct (RAD) to form a right hepatic duct (RHD). (b) Type 2, a triple confluence of the RPD, RAD, and left hepatic bile duct (LHD), joining at the same point to form the common hepatic duct. (c) Type 3, with the RPD draining into the LHD. (d) Type 4, with the RPD draining directly into the common hepatic duct. Note that RPDs in Types 3 and 4 can be called aberrant, because each shows no communication with other biliary segments of the liver.

Table 2. Branching patterns of the right hepatic bile duct

Configuration	Description	Kitami et al [9][a] (n=202)	Chen et al [13][a] (n=56)	Ohkubo et al [8][b] (n=110)
Type 1	Conventional: RPD joining RAD to form RHD	64%	59%	74%
Type 2	Trifurcation	5%	13%	5%
Type 3	RPD joining LHD	17%	9%	12%
Type 4	Aberrant drainage of RPD into CHD	3%	18%	5%
Type 5	Others	11%	2%	4%

CHD, common hepatic bile duct; LHD, left hepatic duct; RAD, right anterior duct; RHD, right hepatid duct; RPD, right posterior duct.
[a]Results of four- or eight-detector row CT.
[b]Results of four- or eight-detector row operative cases.

bile ducts). MIP and VR images are useful for demonstrating insertion of the cystic duct [32]. A long cystic duct paralleling the extrahepatic bile duct (Type A; Figure 5b) is reported in approximately 10% of cholangiograms [29]. The parallel course implies a common fibrous sheath around the cystic duct and CBD, which may cause problems such as inadvertent ligation or transaction of the extrahepatic bile duct at cholecystectomy.

Aberrant bile ducts and accessory bile ducts

Although the terminology used for anomalous bile ducts is confusing, it is surgically significant to distinguish between ''aberrant'' and ''accessory'' bile ducts.

An aberrant bile duct, an anomalous confluence pattern of the hilar bile ducts, is the only bile duct draining a particular segment of the liver (Figure 9) [33], and ligation or dissection of that may result in severe complications.

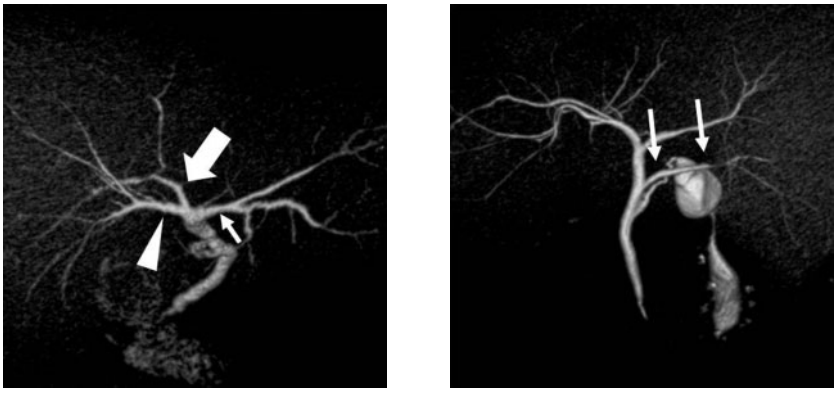

(a) (b)

Figure 5. Patterns of the right hepatic bile duct. (a) A three-dimensional volume-rendering (VR) image (superior oblique view) shows a Type 2 pattern with hilar trifurcation of the right anterior (arrowhead), right posterior (large arrow) and left hepatic (small arrow) ducts. (b) A VR image (posterior view) shows a Type 4 pattern, with aberrant drainage of the right posterior duct into the common hepatic duct (arrows). This case also has Type A cystic duct, as described in Table 3.

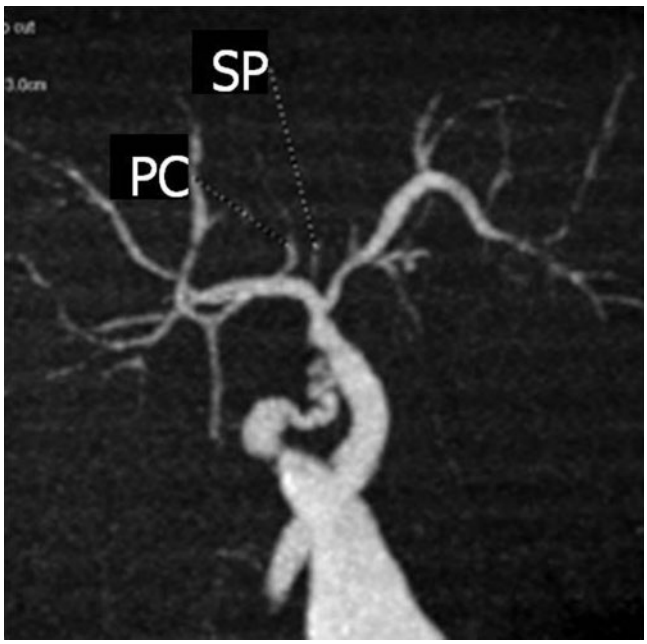

Figure 6. Detection of the bile duct of the caudate lobe on drip infusion cholangiography with CT. A coronal maximum intensity projection image shows the bile duct of the Spiegel lobe (SP) and paracaval portion (PC) draining into the right hepatic duct.

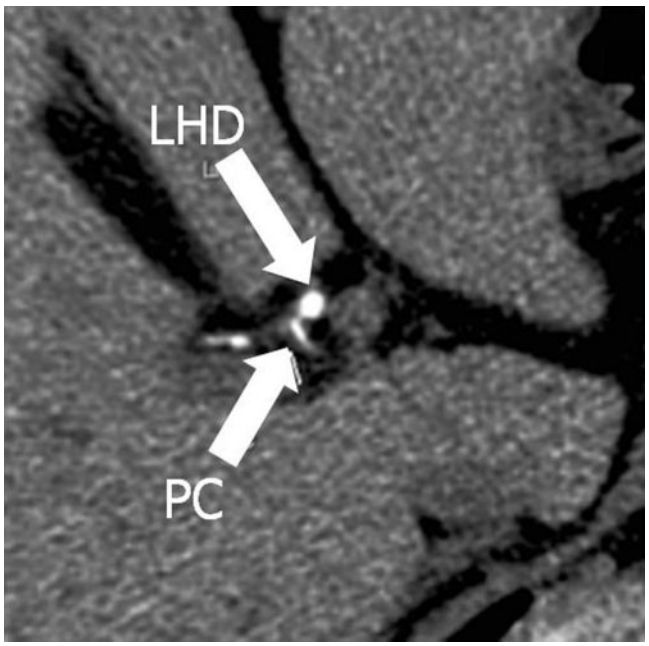

Figure 7. Axial source image (thickness, 0.625 mm) shows the paracaval portion (PC) branch running out of the liver parenchyma in the hepatoduodenal ligament. LHD, left hepatic bile duct.

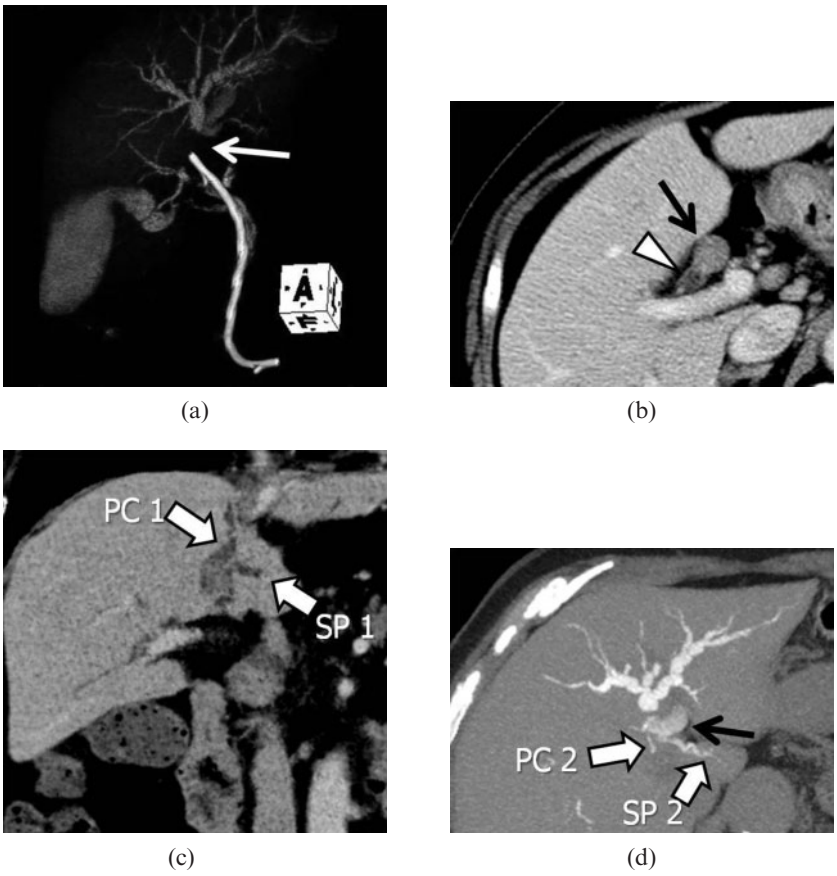

(a) (b) (c) (d)

Figure 8. A case of hilar intraductal cholangiocarcinoma. (a) Volume-rendering image from drip infusion cholangiography with CT (DIC-CT) obtained after stent placement demonstrates obstruction of the proximal left hepatic duct (arrow) with distal dilatation. (b) Axial intravenous contrast-enhanced CT (CECT) indicates tumour occupying the proximal left hepatic duct (arrow), while the right hepatic duct (arrowhead) remains intact. (c) Coronal minimum-intensity projection image of the intravenous CECT demonstrates a dilated paracaval portion branch (PC1) and SP branch (SP1) of the caudate lobe draining into the left hepatic duct. (d) Axial 4.0-mm-thick slab maximum-intensity projection image from DIC-CT depicting other caudate branches (PC2 and SP2) draining into B2 (black arrow). The branching pattern allowed for tumour resection with preservation of the right hepatic lobe.

An accessory bile duct is an additional bile duct draining a particular area of the liver [33]. Ligation of an accessory bile duct does not cause recurrent cholangitis or focal fibrosis of the liver. The subvesical duct (also known as Luschka's duct, the duct of Luschka or the cholecystohepatic duct) is a thin bile duct that passes through the GB fossa, and is one of the causes of self-limiting bile leaks seen after cholecystectomy. This duct is encountered in 1–35% of autopsy specimens [4, 12, 34]. Figure 10 shows a case with both a subvesical duct and an accessory bile duct.

Comparison of drip infusion cholangiography with CT, MR cholangiopancreatography and contrast-enhanced MR cholangiography in evaluation of the biliary tree

Table 4 compares the characteristics of DIC-CT, MRCP and contrast-enhanced MR cholangiography with Gd-EOB-DTPA (EOB-MRC).

Drip infusion cholangiography with CT

The DIC-CT protocol is simple: CT data acquisition 30–60 min after drip infusion of iotroxate meglumine (Biliscopin; Bayer Schering Pharma, Osaka, Japan) assists in visualisation of the biliary tree by biliary excretion of the contrast medium without structural modification. The advent of MDCT has provided high spatial resolution images in a short scanning time. Schroeder et al [35] reported that intra-operative assessment confirmed the pre-operative analysis of branching pattern using DIC-CT in 58 (94%) of 62 living liver donors. Moreover, DIC-CT is also useful for clinical diagnosis and post-operative assessment [3, 17, 28, 32, 36, 37]. In the diagnosis of cholecystolithiasis or choledocholithiasis by DIC-CT, opacification of the biliary tree reveals a radiolucent stone as a filling defect (Figure 11). DIC-CT is considered to provide more reliable information on the location and number of stones than MRCP, since pseudolesion artefacts often appear on MRCP (see the following section on conventional MRCP). Okada et al [32]

Table 3. Variations of the cystic duct

Configuration	Description	Benson and Page [31][a] ($n=140$)
Type A	Long cystic duct with low fusion with common hepatic duct	8.6%
Type B	Abnormally high fusion of cystic duct with common hepatic duct (trifurcation)	2.1%
Type C	Accessory hepatic duct	1.4%
Type D	Cystic duct entering right hepatic duct	0.7%
Type E	Cholecystohepatic duct	0.7%

Benson and Page [31] reported that 65 cadaver cases showed similar incidences of the main duct anomalies.
[a]Results of operative cases.

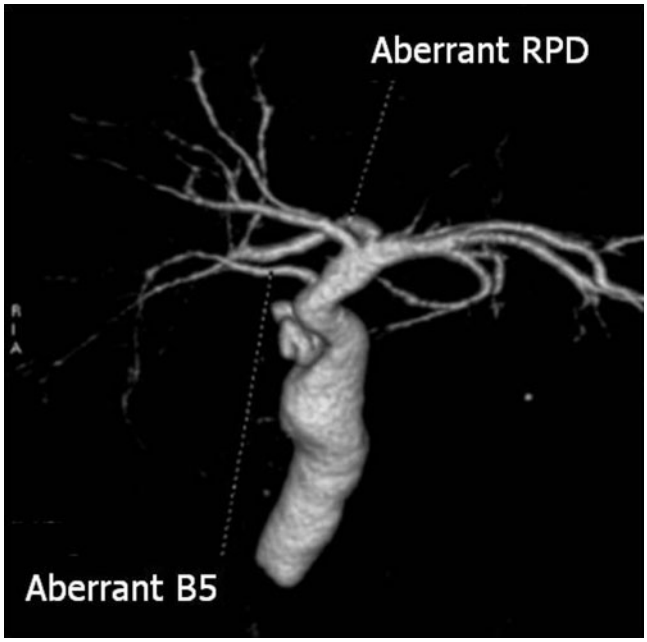

Figure 9. A case with aberrant bile duct and hepatic duct. The three-dimensional volume-rendering image shows an aberrant B5 bile duct draining directly into the common hepatic duct. The aberrant hepatic right posterior duct (aberrant RPD) drains into the left hepatic duct.

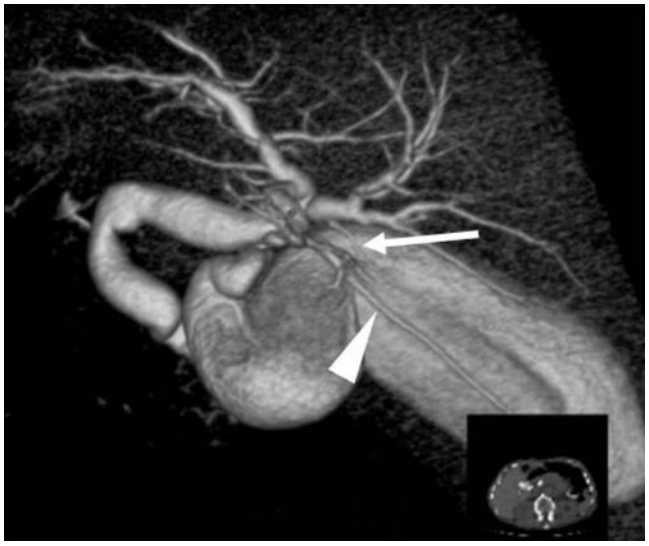

Figure 10. Volume-rendering image (cranial posterior view) of a case with subvesical duct (arrow) draining into the right hepatic duct and an accessory B6 duct (arrowhead) draining into the common hepatic duct. Other branches of the right posterior bile duct drain Segment 6.

described the advantages of DIC-CT over MRCP for detecting intrahepatic bile duct stones.

Visualisation of the bile duct on DIC-CT reflects biliary flow, so we can also assess patency of the bile duct. In post-operative assessment, DIC-CT can detect post-operative bile leaks from the liver stump or from the biliary–enteric anastomosis (Figure 12).

As a technical limitation of DIC-CT, insufficient opacification of the biliary tree is occasionally observed in patients with excessively dilated ducts. Eliminated contrast media often forms fluid–fluid levels in such cases, complicating evaluation of the biliary tree. Furthermore, the biliary tree may be poorly visualised in patients with hyperbilirubinaemia (serum bilirubin $>3\,\mathrm{ml\,dl^{-1}}$), since bilirubin excretion is impaired in such cases [36].

The main disadvantages of DIC-CT compared with MRCP involve the use of radiation and contrast media. Adverse reactions after injection of meglumine iotroxate may occur in 0.8–3.4% of patients [38, 39], although treatment is not usually required: the symptoms typically comprise skin rash, itchy skin, hives or nausea. Persson et al [39] reviewed a total of 4587 patients from 12 previously published studies on the frequency of adverse reactions with infusion of iotroxate for intravenous

Table 4. Comparison of DIC-CT and MR cholangiography

Method	Advantages	Limitations	Indications
DIC-CT	Short scan time	Radiation exposure	Contraindications for MRC (*e.g.* cardiac pacemakers)
	High spatial resolution	Side effects caused by biliary contrast agent (iotroxic acid megulumine)	Pre-operative detailed evaluation of intrahepatic tiny bile duct (caudate, subvesical duct)
	High contrast of biliary tree (including intrahepatic bile duct)	Poor visualisation associated with hyperbilirubinaemia	Post-operative assessment (*e.g.* detection of bile leak)
	Evaluation of biliary flow and function	Insufficient opacification of excessively dilated biliary duct	
MRCP	No contrast agent used	Artefacts and pseudolesions	First choice for pancreaticobiliary diseases, particularly in the investigation of biliary obstruction
	No radiation exposure	Contraindications for MRI	
	High contrast of extrahepatic bile duct		
	Information of pancreatic duct		
EOB-MRC	Biliary flow imaging	No depiction of peripheral bile duct	Additional information about bile duct on ordinary Gd-EOB-DTPA- enhanced liver MRI
		Poor visualisation associated with liver dysfunction	

DIC-CT, drip infusion cholangiography with CT; EOB-MRC, gadolinium ethoxybenzyl diethylenetriamine pentaacetic acid-enhanced MR cholangiography; Gd-EOB-DTPA, gadolinium ethoxybenzyl diethylenetriamine pentaacetic acid; MRCP, MR cholangiopancreatography.

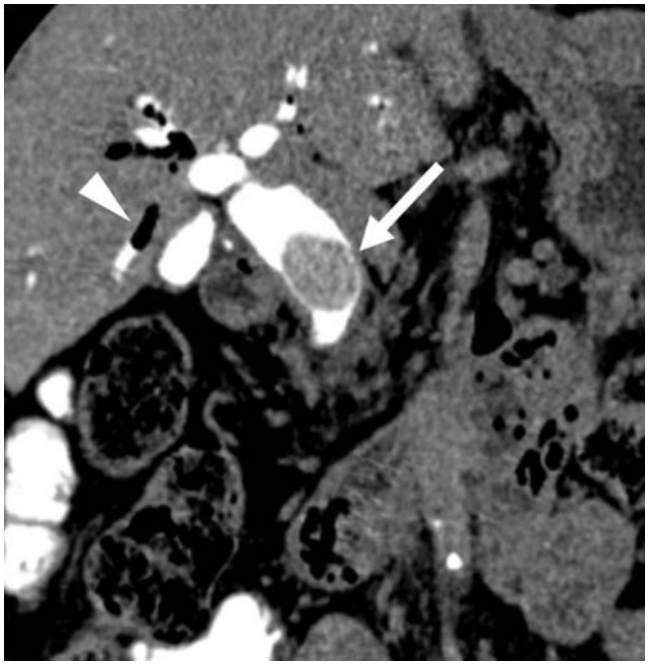

Figure 11. Choledocholithiasis after cholecystectomy. Coronal multiplanar reconstruction (section width, 1.25 mm) of drip infusion cholangiography with CT demonstrates a large stone (arrow) in the common bile duct. Pneumobilia in the right hepatic bile duct (arrowhead) is also recognised.

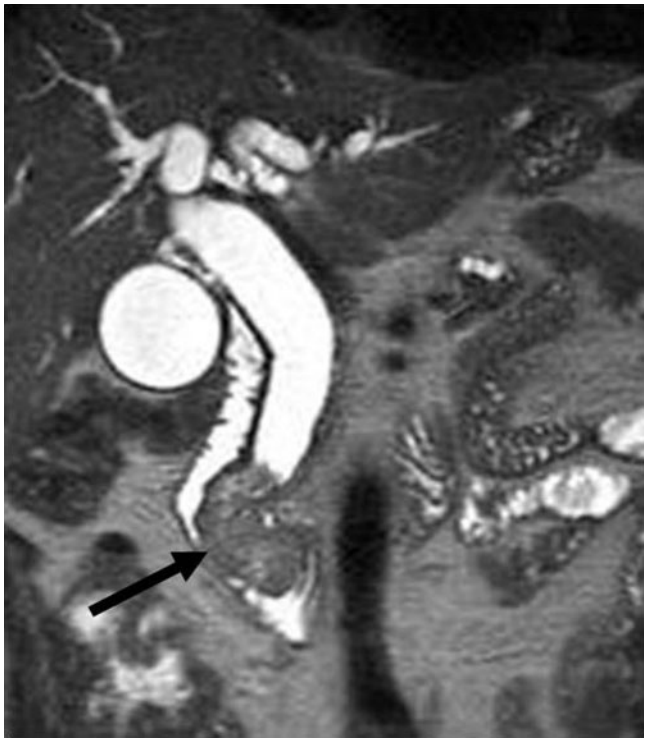

Figure 13. Carcinoma of the papilla of Vater. MR cholangiopancreatography clearly demonstrates obstruction at the level of the distal common hepatic duct and a polypoid lesion located at the papilla of Vater.

cholangiography. They found minor reactions in 1.5–2.2%, intermediate reactions in 1.1–1.8% and severe reactions in 0–0.1%. Thus, the indications for DIC-CT need to be considered from various perspectives: risk of adverse reactions; possibility of failed examination in patients with hyperbilirubinaemia; and the benefit of reducing the risk of bile duct injury during laparoscopic cholecystectomy or liver resection.

Actually, the availability of intravenous cholangiographic contrast medium (Biliscopin; Bayer Schering Pharma, Berlin, Germany) is limited to a few countries. The product information of Biliscopin, generated in 2003, said that the contrast media are sold in five countries: Japan, Germany, the UK, Austria and Australia. The distribution has been decreased recently, and also studies of DIC-CT are becoming less common. The protein-binding characteristics that are essential for biliary contrast media increase the risk of adverse reactions [38, 39], so that better alternative drip-infused biliary contrast media may not be released unless the pharmacological problem is overcome. However, the anatomical knowledge gained through the previous studies using DIC-CT will support clinicians in interpretation of the other cholangiographies (*e.g.* MRCP), and even in intra-operative manoeuvres.

Conventional MR cholangiopancreatography

MRCP enables rapid, non-invasive evaluation of both the biliary tree and pancreatic duct without the use of intravenous contrast media [14, 40, 41]. A much improved spatial and temporal resolution for MRCP data collection has now been achieved, which will enable MR cholangiography to remain the gold standard for evaluation of hepatobiliary disease.

Among the available MRI techniques, the two most commonly used sequences are based on the T_2 weighted

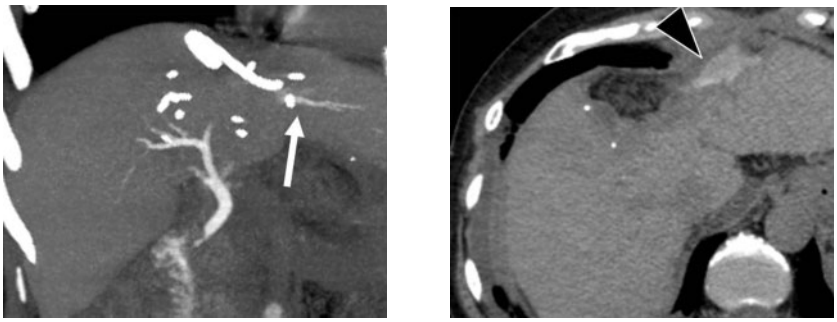

(a) (b)

Figure 12. A 61-year-old female with suspected bile leakage 6 days after hepatic resection (S3 and S4) for hepatocellular carcinoma. Drip infusion cholangiography with CT was performed to detect bile duct injury. (a) On an axial 32-mm-thick slab maximum intensity projection image, the proximal site of B2 (arrow) was not visualised. (b) Axial image demonstrating bile leak from the cut margin of the liver as excreted contrast medium (arrowhead).

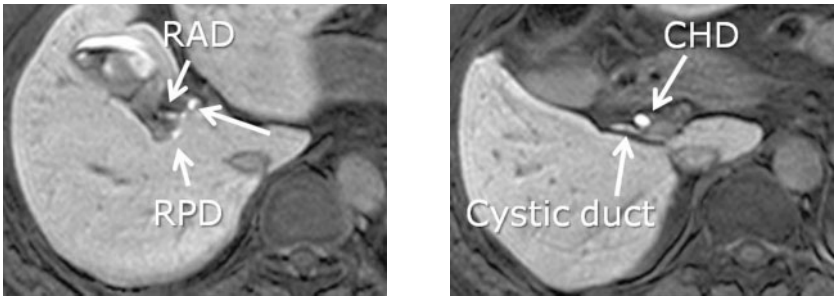

(a) (b)

Figure 14. (a) Ethoxybenzyl-enhanced magnetic resonance cholangiography and (b) axial fat-suppressed 3D T_1 weighted gradient-echo images acquired 20 min after intravenous injection of gadolinium ethoxybenzyl diethylenetriamine pentaacetic acid, depicting the bile ducts. RAD, hepatic right anterior duct; RPD, hepatic right posterior duct; RHD, right hepatic duct; CHD, common hepatic bile duct.

turbo spin-echo sequence [42]: the two-dimensional single-shot fast spin echo (2D SSFSE) sequence; and the respiratory-triggered 3D Fourier transformation fast-recovery fast-spin echo (3D FRFSE) sequence. With 2D SSFSE, the advantage of a shorter acquisition time is balanced against the inability to depict fine details of the biliary tree. Conversely, 3D FRFSE imaging provides high-resolution images of the biliary tree and pancreatic duct in multiple section planes, requiring only 3–4 min of data acquisition time [43]. MRCP at 3.0 T has the potential to depict even greater anatomical detail owing to a higher contrast-to-noise ratio than 1.5 T [44, 45].

One of the best indications for MRCP is biliary obstruction, in contrast to DIC-CT. MRCP can definitively visualise the dilated biliary ducts, and is useful for assessing the level of occlusion in extrahepatic bile ducts [46–48]. Also, the high spatial and contrast resolution provide pre-operative information about the intra- and extrabiliary spread of possible malignant strictures (Figure 13).

Several potential pitfalls must be kept in mind when interpreting MRCP [49]. MRI-specific artefacts may mimic biliary obstruction or choledochal stones (*e.g.* pseudo-obstruction of the common hepatic duct caused by pulsatile vascular compression by the right hepatic artery) [50]. To avoid the pitfalls, conventional MR or contrast-enhanced CT images can provide information regarding adjacent structures such as vessels. Patient-based artefacts, including inadequate breath-holding and excess ascites, should also be recognised.

Contrast-enhanced MR cholangiography with gadolinium ethoxybenzyl diethylenetriamine pentaacetic acid

The benefits of Gd-EOB-DTPA, a liver-specific MRI contrast medium, in the diagnosis of liver tumours have been widely acknowledged [51–55]. Recently, attention has also been focused on the utility in evaluation of the biliary system [47, 56–59]. When Gd-EOB-DTPA is injected intravenously, the contrast medium is incorporated into hepatocytes by the organic anionic transport system after the vascular phase [59]. About 50% of the administered Gd-EOB-DTPA is eliminated as a non-metabolised compound into the biliary tract with mediation by the glutathione-S-transferase transport system, with the remaining 50% excreted via glomerular filtration [60]. The biliary tree can thus be depicted in the hepatobiliary phase (Figure 14). Fat-suppressed 3D T_1 weighted axial images are typically acquired for the hepatobiliary phase [61, 62], and the section thickness is sufficiently thin (1.5–2.0 mm) to allow the generation of MIP images.

Carlos et al [47] were the first to evaluate the clinical efficacy of EOB-MRC, concluding that EOB-MRC as an intrabiliary medium is less widely available than MRCP. It should be recognised that liver function has a huge effect on image quality of Gd-EOB-DTPA-enhanced MRI: Tschirch et al [57] reported that EOB-MRC was sufficient for anatomical visualisation of the biliary tree in 40% of patients with liver cirrhosis, and in 100% of adult individuals with normal liver function. As post-operative evaluation, clinical application of biliary MRI with Gd-EOB-DTPA for detection of bile leaks after biliary surgery or liver trauma has been reported [58, 59].

Conclusion

CT and MR cholangiography are minimally invasive methods that provide precise depiction of the biliary system. DIC-CT allows detailed evaluation of biliary anatomy thanks to the high resolution of images, though the availability of intravenous cholangiographic contrast media is limited to a few countries. MRCP is most widely used as a non-invasive means of evaluating biliary diseases, particularly in patients with dilated bile ducts. Gd-EOB-DTPA-enhanced hepatobiliary phase MRI can delineate the biliary tree and potentially provide additional information regarding biliary flow. Clinicians need to understand the characteristics of each study technique to optimally utilise these methods for perioperative evaluation of biliary tree.

Acknowledgments

Our deepest appreciation goes to Michinobu Nagao and Mark Pavlick for their insightful comments in editing the manuscript.

References

1. Liu CL, Fan ST, Lo CM, Tso WK, Lam CM, Wong J. Improved operative and survival outcomes of surgical treatment for hilar cholangiocarcinoma. Br J Surg 2006; 93:1488–94.
2. Hasegawa S, Ikai I, Fujii H, Hatano E, Shimahara Y. Surgical resection of hilar cholangiocarcinoma: analysis of survival

and postoperative complications. World J Surg 2007; 31:1256–63.
3. Kapoor V, Baron RL, Peterson MS. Bile leaks after surgery. AJR Am J Roentgenol 2004;182:451–8.
4. Suhocki PV, Meyers WC. Injury to aberrant bile ducts during cholecystectomy: a common cause of diagnostic error and treatment delay. AJR Am J Roentgenol 1999; 172:955–9.
5. Endo I, Shimada H, Sugita M, Fujii Y, Morioka D, Takeda K, et al. Role of three-dimensional imaging in operative planning for hilar cholangiocarcinoma. Surgery 2007; 142:666–75.
6. Hekimoglu K, Ustundag Y, Dusak A, Erdem Z, Karademir B, Aydemir S, et al. MRCP vs. ERCP in the evaluation of biliary pathologies: review of current literature. J Dig Dis 2008;9:162–9.
7. Couinaud C. Surgical anatomy of the liver revisited. Paris, France: Coinaud; 1989. pp. 130–2.
8. Ohkubo M, Nagino M, Kamiya J, Yuasa N, Oda K, Arai T, et al. Surgical anatomy of the bile ducts at the hepatic hilum as applied to living donor liver transplantation. Ann Surg 2004;239:82–6.
9. Kitami M, Takase K, Murakami G, Ko S, Tsuboi M, Saito H, et al. Types and frequencies of biliary tract variations associated with a major portal venous anomaly: analysis with multi-detector row CT cholangiography. Radiology 2006;238:156–66.
10. Cho A, Okazumi S, Yoshinaga Y, Ishikawa Y, Ryu M, Ochiai T. Relationship between left biliary duct system and left portal vein: evaluation with three-dimensional porto-cholangiography. Radiology 2003;228:246–50.
11. Kawarada Y, Das BC, Onishi H, Taoka H, Gadzijev EM, Ravnik D, et al. Surgical anatomy of the bile duct branches of the medial segment (B4) of the liver in relation to hilar carcinoma. J Hepatobiliary Pancreat Surg 2000;7:480–5.
12. Kitami M, Murakami G, Suzuki D, Takase K, Tsuboi M, Saito H, et al. Heterogeneity of subvesical ducts or the ducts of Luschka: a study using drip-infusion cholangiography-computed tomography in patients and cadaver specimens. World J Surg 2005;29:217–23.
13. Chen JS, Yeh BM, Wang ZJ, Roberts JP, Breiman RS, Qayyum A, et al. Concordance of second-order portal venous and biliary tract anatomies on MDCT angiography and MDCT cholangiography. AJR Am J Roentgenol 2005;184:70–4.
14. Limanond P, Raman SS, Ghobrial RM, Busuttil RW, Lu DS. The utility of MRCP in preoperative mapping of biliary anatomy in adult-to-adult living related liver transplant donors. J Magn Reson Imaging 2004;19:209–15.
15. Gazelle GS, Lee MJ, Mueller PR. Cholangiographic segmental anatomy of the liver. Radiographics 1994;14: 1005–13.
16. Cheng YF, Huang TL, Chen CL, Sheen-Chen SM, Lui CC, Chen TY, et al. Anatomic dissociation between the intrahepatic bile duct and portal vein: risk factors for left hepatectomy. World J Surg 1997;21:297–300.
17. Hirao K, Miyazaki A, Fujimoto T, Isomoto I, Hayashi K. Evaluation of aberrant bile ducts before laparoscopic cholecystectomy: helical CT cholangiography versus MR cholangiography. AJR Am J Roentgenol 2000;175:713–20.
18. Murakami T, Kim T, Tomoda K, Narumi Y, Sakon M, Monden M, et al. Aberrant right posterior biliary duct: detection by intravenous cholangiography with helical CT. J Comput Assist Tomogr 1997;21:733–4.
19. Lee VS, Morgan GR, Teperman LW, John D, Diflo T, Pandharipande PV, et al. MR imaging as the sole preoperative imaging modality for right hepatectomy: a prospective study of living adult-to-adult liver donor candidates. AJR Am J Roentgenol 2001;176:1475–82.
20. Lee UY, Murakami G, Han SH. Arterial supply and biliary drainage of the dorsal liver: a dissection study using controlled specimens. Anat Sci Int 2004;79:158–66.
21. Filipponi F, Romagnoli P, Mosca F, Couinaud C. The dorsal sector of human liver: embryological, anatomical and clinical relevance. Hepatogastroenterology 2000;47:1726–31.
22. Kumon M. Anatomy of the caudate lobe with special reference to portal vein and bile duct. Acta Hepat Jan 1985;26:1193–8.
23. Bartlett D, Fong Y, Blumgart LH. Complete resection of the caudate lobe of the liver: technique and results. Br J Surg 1996;83:1076–81.
24. Furukawa H, Sano K, Kosuge T, Shimada K, Yamamoto J, Ishii H, et al. Analysis of biliary drainage in the caudate lobe of the liver: comparison of three-dimensional CT cholangiography and rotating cine cholangiography. Radiology 1997;204:113–17.
25. Murakami G, Hata F. Human liver caudate lobe and liver segment. Anat Sci Int 2002;77:211–24.
26. Wen ZQ, Yan YQ, Yang JM, Wu MC. Precautions in caudate lobe resection: report of 11 cases. World J Gastroenterol 2008;14:2767–70.
27. Yamamoto T, Kubo S, Shuto T, Ichikawa T, Ogawa M, Hai S, et al. Surgical strategy for hepatocellular carcinoma originating in the caudate lobe. Surgery 2004;135:595–603.
28. Takamatsu S, Goseki N, Nakajima K, Teramoto K, Iwai T, Arii S. Distributing pattern of the bile duct of the caudate lobe on computed tomography with drip infusion cholangiography and its surgical significance. Hepatogastroenterology 2004; 51:29–32.
29. Turner MA, Fulcher AS. The cystic duct: normal anatomy and disease processes. Radiographics 2001;21:3–22; questionnaire 288–94.
30. Kwon AH, Uetsuji S, Ogura T, Kamiyama Y. Spiral computed tomography scanning after intravenous infusion cholangiography for biliary duct anomalies. Am J Surg 1997;174:396–401; discussion 401–2.
31. Benson EA, Page RE. A practical reappraisal of the anatomy of the extrahepatic bile ducts and arteries. Br J Surg 1976;63:853–60.
32. Okada M, Fukada J, Toya K, Ito R, Ohashi T, Yorozu A. The value of drip infusion cholangiography using multidetector-row helical CT in patients with choledocholithiasis. Eur Radiol 2005;15:2140–5.
33. Mortele KJ, Ros PR. Anatomic variants of the biliary tree: MR cholangiographic findings and clinical applications. AJR Am J Roentgenol 2001;177:389–94.
34. Ko K, Kamiya J, Nagino M, Oda K, Yuasa N, Arai T, et al. A study of the subvesical bile duct (duct of Luschka) in resected liver specimens. World J Surg 2006;30:1316–20.
35. Schroeder T, Radtke A, Kuehl H, Debatin JF, Malago M, Ruehm SG. Evaluation of living liver donors with an all-inclusive 3D multi-detector row CT protocol. Radiology 2006;238:900–10.
36. Stockberger SM, Wass JL, Sherman S, Lehman GA, Kopecky KK. Intravenous cholangiography with helical CT: comparison with endoscopic retrograde cholangiography. Radiology 1994;192:675–80.
37. Hashimoto M, Itoh K, Takeda K, Shibata T, Okada T, Okuno Y, et al. Evaluation of biliary abnormalities with 64-channel multidetector CT. Radiographics 2008;28:119–34.
38. Nilsson U. Adverse reactions to iotroxate at intravenous cholangiography. A prospective clinical investigation and review of the literature. Acta Radiol 1987;28:571–5.
39. Persson A, Dahlstrom N, Smedby O, Brismar TB. Three-dimensional drip infusion CT cholangiography in patients with suspected obstructive biliary disease: a retrospective analysis of feasibility and adverse reaction to contrast material. BMC Med Imaging 2006;6:1.

40. Fulcher AS, Turner MA. HASTE MR cholangiography in the evaluation of hilar cholangiocarcinoma. AJR Am J Roentgenol 1997;169:1501–5.
41. Figueras J, Llado L, Valls C, Serrano T, Ramos E, Fabregat J, et al. Changing strategies in diagnosis and management of hilar cholangiocarcinoma. Liver Transpl 2000;6:786–94.
42. Morita S, Saito N, Suzuki K, Mitsuhashi N. Biliary anatomy on 3D MRCP: comparison of volume-rendering and maximum-intensity-projection algorithms. J Magn Reson Imaging 2009;29:601–6.
43. Fulcher AS, Turner MA, Capps GW. MR cholangiography: technical advances and clinical applications. Radiographics 1999;19:25–41; discussion 41–4.
44. Isoda H, Kataoka M, Maetani Y, Kido A, Umeoka S, Tamai K, et al. MRCP imaging at 3.0 T vs. 1.5 T: preliminary experience in healthy volunteers. J Magn Reson Imaging 2007;25:1000–6.
45. Onishi H, Kim T, Hori M, Murakami T, Tatsumi M, Nakaya Y, et al. MR cholangiopancreatography at 3.0 T: intraindividual comparative study with MR cholangiopancreatography at 1.5 T for clinical patients. Invest Radiol 2009;44:559–65.
46. Soto JA, Barish MA, Yucel EK, Siegenberg D, Ferrucci JT, Chuttani R. Magnetic resonance cholangiography: comparison with endoscopic retrograde cholangiopancreatography. Gastroenterology 1996;110:589–97.
47. Carlos RC, Hussain HK, Song JH, Francis IR. Gadolinium-ethoxybenzyl-diethylenetriamine pentaacetic acid as an intrabiliary contrast agent: preliminary assessment. AJR Am J Roentgenol 2002;179:87–92.
48. Wallner BK, Schumacher KA, Weidenmaier W, Friedrich JM. Dilated biliary tract: evaluation with MR cholangiography with a *T*2-weighted contrast-enhanced fast sequence. Radiology 1991;181:805–8.
49. Irie H, Honda H, Kuroiwa T, Yoshimitsu K, Aibe H, Shinozaki K, et al. Pitfalls in MR cholangiopancreatographic interpretation. Radiographics 2001;21:23–37.
50. Watanabe Y, Dohke M, Ishimori T, Amoh Y, Okumura A, Oda K, et al. Pseudo-obstruction of the extrahepatic bile duct due to artifact from arterial pulsatile compression: a diagnostic pitfall of MR cholangiopancreatography. Radiology 2000;214:856–60.
51. Bluemke DA, Sahani D, Amendola M, Balzer T, Breuer J, Brown JJ, et al. Efficacy and safety of MR imaging with liver-specific contrast agent: U.S. multicenter phase III study. Radiology 2005;237:89–98.
52. Huppertz A, Haraida S, Kraus A, Zech CJ, Scheidler J, Breuer J, et al. Enhancement of focal liver lesions at gadoxetic acid-enhanced MR imaging: correlation with histopathologic findings and spiral CT—initial observations. Radiology 2005;234:468–78.
53. Reimer P, Rummeny EJ, Daldrup HE, Hesse T, Balzer T, Tombach B, et al. Enhancement characteristics of liver metastases, hepatocellular carcinomas, and hemangiomas with Gd-EOB-DTPA: preliminary results with dynamic MR imaging. Eur Radiol 1997;7:275–80.
54. Vogl TJ, Kummel S, Hammerstingl R, Schellenbeck M, Schumacher G, Balzer T, et al. Liver tumors: comparison of MR imaging with Gd-EOB-DTPA and Gd-DTPA. Radiology 1996;200:59–67.
55. Kogita S, Imai Y, Okada M, Kim T, Onishi H, Takamura M, et al. Gd-EOB-DTPA-enhanced magnetic resonance images of hepatocellular carcinoma: correlation with histological grading and portal blood flow. Eur Radiol 2010;20:2405–13.
56. Bollow M, Taupitz M, Hamm B, Staks T, Wolf KJ, Weinmann HJ. Gadolinium-ethoxybenzyl-DTPA as a hepatobiliary contrast agent for use in MR cholangiography: results of an in vivo phase-I clinical evaluation. Eur Radiol 1997;7:126–32.
57. Tschirch FT, Struwe A, Petrowsky H, Kakales I, Marincek B, Weishaupt D. Contrast-enhanced MR cholangiography with Gd-EOB-DTPA in patients with liver cirrhosis: visualization of the biliary ducts in comparison with patients with normal liver parenchyma. Eur Radiol 2008;18:1577–86.
58. Seale MK, Catalano OA, Saini S, Hahn PF, Sahani DV. Hepatobiliary-specific MR contrast agents: role in imaging the liver and biliary tree. Radiographics 2009;29:1725–48.
59. Lee NK, Kim S, Lee JW, Lee SH, Kang DH, Kim GH, et al. Biliary MR imaging with Gd-EOB-DTPA and its clinical applications. Radiographics 2009;29:1707–24.
60. Schuhmann-Giampieri G, Schmitt-Willich H, Frenzel T, Schitt-Willich H. Biliary excretion and pharmacokinetics of a gadolinium chelate used as a liver-specific contrast agent for magnetic resonance imaging in the rat. J Pharm Sci 1993;82:799–803.
61. Reimer P, Schneider G, Schima W. Hepatobiliary contrast agents for contrast-enhanced MRI of the liver: properties, clinical development and applications. Eur Radiol 2004;14:559–78.
62. Zech CJ, Herrmann KA, Reiser MF, Schoenberg SO. MR imaging in patients with suspected liver metastases: value of liver-specific contrast agent Gd-EOB-DTPA. Magn Reson Med Sci 2007;6:43–52.